

N O T I C E

THIS DOCUMENT HAS BEEN REPRODUCED FROM
MICROFICHE. ALTHOUGH IT IS RECOGNIZED THAT
CERTAIN PORTIONS ARE ILLEGIBLE, IT IS BEING RELEASED
IN THE INTEREST OF MAKING AVAILABLE AS MUCH
INFORMATION AS POSSIBLE

NI

**The Two-Photon Absorptivity
of Rotational Transitions in the
 $A^2\Sigma^+ (v' = 0) - X^2\Pi (v'' = 0)$
Gamma Band of Nitric Oxide**

K. P. Gross and R. L. McKenzie

(NASA-TM-81335) THE TWO-PHOTON ABSORPTIVITY
OF ROTATIONAL TRANSITIONS IN THE A2 SIGMA
HYPERON + (V PRIME = 0) - X-2 PION (V PRIME
PRIME = 0) GAMMA BAND OF NITRIC OXIDE (NASA)
28 p HC A03/MF A01

N82-16815

Unclas
08866

CSCI 20:1 G3/72

January 1982



The Two-Photon Absorptivity of Rotational Transitions in the $A^2\Sigma^+ (v' = 0) - X^2\Pi (v'' = 0)$ Gamma Band of Nitric Oxide

K. P. Gross, Stanford University, Stanford, California
R. L. McKenzie, Ames Research Center, Moffett Field, California

NASA

National Aeronautics and
Space Administration

Ames Research Center
Moffett Field California 94035

The two-photon absorptivity of rotational transitions in
the $A^2\Sigma^+(v' = 0) - X^2\Pi(v'' = 0)$ gamma band of nitric oxide

K. P. Gross^a

*Stanford University, Department of Aeronautics and Astronautics,
Stanford, California 94305*

and

R. L. McKenzie

Ames Research Center, NASA, Moffett Field, California 94035

(Received

A predominantly single-mode pulsed dye laser system giving a well-characterized spatial and temporal output suitable for absolute two-photon absorptivity measurements was used to study the NO $\gamma(0,0) S_{11} + R_{21}$ ($J'' = 7-1/2$) transition. Using a calibrated induced-fluorescence technique, an absorptivity parameter of $2.8 \pm 1.4 \times 10^{-51} \text{ cm}^6$ was obtained. Relative strengths of other rotational transitions in the $\gamma(0,0)$ band were also measured and shown to compare well with predicted values in all cases except the O_{12} ($J'' = 10-1/2$) transition.

^aPermanent address: Mail Stop 230-3, Ames Research Center, NASA, Moffett Field, California 94035.

I. INTRODUCTION

Two-photon absorption in NO has been shown to offer a practical means of measuring fluctuating temperatures in cold turbulent flows seeded with trace concentrations of the absorber.¹ In support of that work, we report here a measurement of the absolute two-photon absorptivity for rotational transitions in the NO $\gamma(0,0)$ band and we describe some studies of its fluorescence-excitation spectrum. Our approach for characterizing the entire band is to first confirm the accuracy of a theoretical model for the relative rotational transition strengths and then to scale the predicted absorptivities, using an absolute measurement of one of the strongest isolated lines in the band.

In the sections to follow, two separate laser systems are described. The first is a relatively simple system that is suitable for scanning. It was used to obtain relative line strengths and spectral positions in several regions of the spectrum where individual rotational transitions are most easily resolved. The results are compared with predictions based on rotational line-intensity factors from an intermediate-coupling model for two-photon transitions, developed by Halpern *et al.*² We then describe a second experiment to measure the absolute absorptivity of the $S_{11} + R_{21}$ ($J'' = 7-1/2$) transition, using a predominantly single-mode pulsed dye laser that minimizes experimental uncertainties due to indeterminate temporal and spectral effects. Our measurement is compared with the only other two-photon absorptivity measurement for NO known to us, that obtained by Hochstrasser *et al.*³ from a three-wave mixing experiment.

II. ROTATIONAL SPECTRUM STUDIES

A. Experimental description

To confirm both the recent theoretical model of Halpern *et al.*¹ for predicting relative line strengths and the established term coefficients for predicting relative spectral positions, we first scanned the selected regions of the spectrum shown in Fig. 1. A Molelectron DL-200 dye laser pumped by a nitrogen laser was used, giving 5-ns pulses of 50-100 μJ . Laser linewidths were typically 0.3 cm^{-1} . The average pulse energy was maintained at a near-constant value over the scanning range from 448 to 455 nm by manually adjusting the pump energy. Following each laser pulse, broadband fluorescence in the spectral range from 225 to 330 nm, from the $A^2\Sigma^+$ ($v' = 0$) state, was detected on an optical axis at 90° to the focused laser beam. The detection system consisted of $f/1.2$ fused-silica optics followed by a Schott UG-5 absorption filter and an EMI CsTe solar-blind photomultiplier. Signals were integrated and averaged with a PAR 164/162 boxcar integrator.

B. Relative line strengths

The spectral regions studied in detail here complement similar investigations by Halpern *et al.*,² who reported the relative strengths of rotational transitions in the O_{11} branch of $\text{NO } \gamma(0,0)$, and by Bray and Hochstrasser,³ who studied the O_{12} branch. An example of our measurement is shown in Fig. 2 for the spectrum in a region dominated by overlapping R and S branches. Measured relative peaks compare exceptionally well with the synthetic spectrum generated using Halpern's intensity factors. The results of more specific measurements, in which extensive signal

averaging at each of the line peaks was performed, are shown in Fig. 3 for selected transitions in the $S_{11} + R_{21}$ branch. Theory and experiment agree within the experimental uncertainty over a wide range of initial rotational states.

Similar results were obtained for the O_{12} branch, with the exception of the $J'' = 10-1/2$ transition. A comparison of the experimental and predicted spectra for near collision-free conditions is shown in Fig. 4. The absorptivity of the $J'' = 10-1/2$ transition consistently was found to be approximately one half of its predicted value, at least as measured by monitoring fluorescence from the $A^2\Sigma^+$ ($v' = 0$) state. Efforts to remove possible impurities made no difference; but, as cell pressure was increased, either by adding NO or N_2 , the apparent absorptivity increased toward its predicted value. Equivalent observations have been reported by others.^{4,5} We also found that by decreasing the laser linewidth to approximately 0.1 cm^{-1} , peak absorptivities approaching the predicted value were obtained at all cell pressures.

Finally, additional anomalous line peaks were found in the O_{12} branch of the $\gamma(0,1)$ band for the $J'' = 8-1/2$ and $12-1/2$ transitions, with similar behavior caused by variations in pressure and laser linewidth. Subsequent experiments were performed using two synchronously pumped dye lasers, each at a different nonresonant frequency, but with their sum equal to the $\gamma(0,0)$ O_{12} branch two-photon resonance. With that mode of excitation, the effect was completely absent, giving experimental and predicted spectra that matched well for all transitions at any cell pressure. A possible explanation of the causes for these anomalous line

absorptivities has recently been offered,⁵ but the details still appear to warrant further study.

C. Spectral positions

In addition to the line-strength studies, relative spectral positions of individual rotational transitions obtained from our spectra and from the very high resolution scans of Wallenstein and Zacharias⁶ were compared with term values from the recent literature.^{7,8} The comparisons reveal that two-photon fluorescence excitation spectra offer enhanced sensitivity for determining the rotational term coefficients over conventional single-photon emission or absorption spectroscopy. The additional sensitivity is due to the presence of overlapping R and S branches containing easily resolved transitions from large values of J'' . As a result, we found that the term expressions formulated from the intermediate-coupling model of Engleman and Rouse⁷ provided an adequate spectral model, but their coefficients were not sufficiently accurate to reproduce the relative positions of large J'' transitions in the overlapping R and S branches. In fact, relative line positions were transposed in some cases, and corrections could only be made by adjusting the fundamental rotational constants, B_v , and $B_{v''}$. Reasonable changes to higher-order coefficients were not adequate. Since our initial comparisons, Freedman and Nicholls⁸ have reanalyzed Engleman's data and have also made adjustments to the rotational constants. We find now that the use of the coefficients from Freedman and Nicholls⁸ and the term expressions from Engleman and Rouse⁷ reproduces our experimental spectra within the resolution of the data in all regions of the $\gamma(0,0)$ band studied.

As Ref. 1 describes, the R, S region is of greatest interest for our thermometry application. The studies discussed in this section have confirmed that relative two-photon rotational absorptivities in that region are generally well behaved and can be described with apparent accuracy by the intermediate-coupling models tested.^{2,7,8} With those results, one then needs only to determine the absolute absorptivity of a single transition to scale the entire spectrum.

III. ABSOLUTE $S_{11} + R_{21}$ ($J'' = 7-1/2$) ABSORPTIVITY

A. Definition of parameters

The absolute measurement of a multiphoton process is always done with greater risk of inaccuracy than its single-photon equivalent because of the quadratic dependence on spatial, temporal, and spectral properties of the incident beam. Thus, to identify the essential attributes of an experiment in which the uncertainties are minimized, we first define the experimental parameters associated with two-photon absorptivity and the effects of their uncertainties on its measurement. Of particular interest are the field-correlation and spectral properties of the laser related to its axial modes.

As derived in Ref. 1, the two-photon absorptivity for an unsaturated transition between lower and upper states, $|l\rangle \rightarrow |u\rangle$, may be evaluated in terms of the experimental parameters by the coefficient,

$$\alpha_{ul}^{(2)} = \left(1 + \frac{\tau_f}{\tau_c} \right) \frac{E_f/Q_L}{A_0 LN_l}, \quad [\text{cm}^4/\text{J}] \quad (1)$$

where τ_f and τ_c are the fluorescence lifetime and the collisional decay time respectively, E_f is the total fluorescence energy emitted

following excitation, A_0 is a characteristic laser beam cross-sectional area conveniently evaluated at the focused beam waist, L is the axial length of the beam viewed by the fluorescence detector, and N_L is the initial number density of absorbers in the lower state. The experimentally dependent parameter, Q_L , contains all of the information describing the two-photon interaction of the incident beam with the absorbing gas. Equation (1) is valid for cases in which the laser field duration is short compared with the decay time of the upper state but long compared with its collisional dephasing time. In any case, $\alpha_{ul}^{(2)}$ may be related to the molecular properties of the absorber through a two-photon matrix element according to¹

$$|M_{ul}|^2 = \frac{\hbar^2 c^2}{4\pi^3 \hbar \omega_{ul}} \alpha_{ul}^{(2)}, \quad [\text{cm}^6] \quad (2)$$

where $\hbar \omega_{ul}$ is the transition energy. In contrast to Eq. (2), a two-photon absorption parameter appearing often in the literature is defined by

$$\delta_{ul} = \frac{8\pi^3}{c^2} \omega_L^2 g(\omega_{ul} - 2\omega_L) G^{(2)} |M_{ul}|^2, \quad [\text{cm}^4\text{-sec/photon}] \quad (3)$$

where ω_L is a monochromatic laser frequency, $g(\omega_{ul} - 2\omega_L)$ is the transition line-shape function, and $G^{(2)}$ is a second-order field correlation or coherence function. However, δ_{ul} implicitly contains the dependence of the line-shape function on the experimental conditions, and it is applicable only if the spectral width of the laser is very narrow compared with that of the absorbing transition, as with a single-mode laser.

Regardless of the absorptivity parameter used, the accuracy of its measurement will depend on a determination of Q_L , defined in general for a single-beam experiment as

$$Q_L = \bar{g}G^{(2)} \frac{\phi_L}{A_0^2} \int P_L^2(t) dt , \quad (4)$$

where ϕ_L is a focusing function that describes the field intensity variation along the beam axis, $P_L(t)$ is the time-dependent laser power, and the integral extends over the duration of the laser pulse. The product, $\bar{g}G^{(2)}$, describes the combined, and sometimes inseparable, effects of temporal coherence and the convolved spectral distributions for the incident beam and the absorbing transition.

The convolution integral may be written in general terms as

$$\bar{g} = \int_{-\infty}^{\infty} \int_{-\infty}^{\infty} g(\omega_{ul} - \omega - \omega') g_L(\omega_L - \omega) g_L(\omega_L - \omega') d(\omega_L - \omega) d(\omega_L - \omega') \quad (5)$$

where $g(\omega_{ul} - \omega - \omega')$ is the normalized transition line-shape function centered at ω_{ul} , and $g_L(\omega_L - \omega)$ is the normalized frequency distribution for the laser centered at ω_L . Typically, however, $g_L(\omega_L - \omega)$ is not a continuous function but a composite of axial modes appearing as delta functions under a gain-envelope. Under those conditions, $G^{(2)}$ can have a different value for the interaction between each pair of modes. For fields with one or more statistically independent modes, $G^{(2)}$ can range from a value of unity for the self-interaction (auto-correlation) of each mode to a value of 2 for the chaotic interaction (cross-correlation) of uncorrelated pairs.⁹⁻¹²

Of all of the parameters in Eqs. (1) and (4) requiring evaluation to obtain $\alpha_{ul}^{(2)}$, control of the product $\bar{g}G^{(2)}$ places the greatest demands on the laser performance. The least ambiguous case is that of a single-beam experiment with a single axial mode. The auto-correlation function is then equal to unity and Eq. (5) reduces to $\bar{g} = g(\omega_{ul} - 2\omega_L)$. However, even the short cavity length of our dye oscillator occasionally allowed adjacent modes to oscillate simultaneously. Typically they are uncorrelated,⁹ giving a cross-correlation function $G^{(2)} = 2$ in the extreme case. In any case, the effect of multimode uncertainties on the product $\bar{g}G^{(2)}$ is not large if the laser is constrained to just a few modes.

To illustrate the size of their effect, sample calculations are summarized in Table I for the single-mode case and for the multimode patterns seen most frequently in our experiment. The transition line-shape function, including the influence of collision broadening for a cell pressure of 115 Torr, is represented by the Voigt function data, and the Doppler-function data represent negligible collisional broadening. Voigt parameters used for the NO $\gamma(0,0)$ band were taken from Ref. 13. The total intensity in all modes is the same for each pattern. Table I shows that although the absorption is strongly dependent on the transition linewidth, it is only weakly affected by the variations in mode patterns. Furthermore, the ratio of absorption for collision-broadened and Doppler-broadened conditions, averaged over many pulses, can provide an indication of the degree to which the laser is operating with a single axial mode.

The spatial properties of the incident beam, represented by ϕ_L and A_0 in Eq. (4) are also required to determine Q_L . Their evaluation is

least ambiguous for a diffraction-limited beam in the lowest-order transverse mode. For example, in the absence of saturation, the focusing function for spherical waves with a Gaussian variation in amplitude transverse to the beam axis is known to be

$$\phi_L = \frac{\tan^{-1}(L/2b)}{L/2b} \quad (6)$$

where $b = A_0 \omega_L / c$ is the confocal parameter, L is the length of beam centered on the focal point that is viewed by the collection optics, and A_0 is the minimum area of the focused beam defined by the radius at $1/e^2$ of the peak intensity. For $2b/L \ll 1$ (small A_0), $\alpha_{ul}^{(2)}$ becomes insensitive to A_0 making an accurate knowledge of its value unimportant. In practice, A_0 was measured using a series of calibrated apertures.

The remaining parameters in Eqs. (1) and (4) reduce to the ratio, $E_f / \int P_L^2 dt$. Although its elements may each be measured directly, in practice this ratio contributed the largest uncertainty to the evaluation of $\alpha_{ul}^{(2)}$. In our experiments, it was obtained by simultaneously recording the fluorescence and laser temporal waveforms for each laser pulse using transient digitizers. The waveforms were then integrated, ratioed, and averaged over a large number of pulses. Again, the single-mode nature of the laser enhanced the accuracy of this process, because it provided a smoothly varying laser waveform that was easily resolved by the bandwidth of the detector and recording electronics. However, even after rejecting multimode and anomalous waveforms, we still experienced a 25% uncertainty for the average value of the ratio when comparing measurements made at different times. This result, which is a manifestation of several

residual effects, including laser frequency drift from the line peak and the low intrinsic signal-to-noise ratio of the detected fluorescence signals, may be compared with the uncertainty in normalizing the linear power integral, $\int P_L(t)dt$, by the laser pulse energy measured directly with a joulemeter. In that exercise an uncertainty of only a few percent resulted.

B. Experimental arrangement

A schematic of the dye laser and fluorescence data acquisition system is shown in Fig. 5. The pump beam was the third-harmonic output of a Quanta-Ray DCR-1A Nd:YAG laser equipped with a harmonic generator and electronic line-narrowing (ELN) device.¹⁴ The Nd:YAG system was operated at 10 Hz to produce 10 mJ pulses at 355 nm with durations of 6-8 nsec. Over half were single-axial-mode pulses with Gaussian-like waveforms controlled by the ELN. The smoothness of the pump pulse was an essential aspect of the experiment that insured our ability to temporally resolve the waveform of the dye laser and improve the stability of its single mode operation. The dye oscillator had a dual-grating grazing incidence configuration similar to the design of others.^{15,16} A mixture of Coumarin 1 and 2 in ethanol was transversely excited in flowing dye cells to obtain oscillation at wavelengths in the range centered at 452 nm. The oscillator was constrained to (predominately) one axial mode by the spectral bandwidth of the dual-grating arrangement. However, further enhancement was obtained by double-pumping the dye in a manner analogous to the ELN scheme.¹⁴ A preconditioning pump pulse arrived first and started oscillation near threshold on the mode with highest gain. One cavity round-trip

time later, a second pump pulse added energy to the oscillating mode. The output was then amplified and spatially filtered using a direct vision prism and pinhole aperture.¹⁷ The filtering suppressed superradiance to less than 1% of the pulse energy. Typical pulse energies were 10 μJ in 2-4 nsec. Spectral widths were less than 0.02 cm^{-1} FWHM for a single axial mode based on the resolution limit of our Fabry-Perot analyzer. However, some mode variations and spectral jitter occurred that contributed to the uncertainty of our final measurement.

The nitric oxide sample cell was a 5-cm diameter Pyrex-pipe cross with internal f/1.2 fused-silica collection optics. The focused laser beam was polarized perpendicular to the plane of observation, with its observed axial length limited by an aperture at the second focal point ahead of the same filter/photomultiplier combination used in the scanning experiments. The waveform of each laser pulse was monitored with a Hamamatsu biplanar photodiode having a 300 psec rise time, and its integral was calibrated with a Molectron J3-05 pyroelectric joulemeter. The fluorescence and laser waveforms for each pulse were recorded by two Tektronix 7912AD transient digitizers and stored on magnetic disc by an HP1000 computer system. The fluorescence detection system was calibrated radiometrically by filling the sample cell with a variety of gases having well-known Rayleigh scattering cross sections¹⁸ and measuring the Rayleigh scattering energy at 266 nm from the Nd:YAG fourth harmonic. The calibration was corrected for the spectral response of the photomultiplier and filter combination to correspond to fluorescence in the range from 225-330 nm. Before each run, the dye laser was tuned to the peak of the

$S_{11} + R_{21}$ ($J'' = 7-1/2$) transition and optimized for single-mode operation by monitoring the Fabry-Perot fringe pattern on an optical multichannel analyzer. The axial mode spacing was 0.05 cm^{-1} , and the frequency jitter associated with each mode was less than 0.01 cm^{-1} . During a run, data from 200 successive pulses could be recorded and stored.

C. Absorptivity measurement

To test the accuracy of the measurements, several aspects of the experimental system were first verified. For example, the absence of unresolved temporal structure in the dye laser waveforms was confirmed by monitoring the pulses with direct-access electronics having an overall rise time of 400 psec. The waveforms continued to appear to be slowly varying over their duration. The linearity of the system was verified by testing the dependence of average fluorescence energy on the NO number density, the focal area, and the square of the average laser power. Variations following those expected according to Eq. (1) were observed in all cases within an experimental uncertainty of 10%. Those results, along with the good agreement between predicted and experimental relative line intensities, were also taken to indicate the absence of saturation effects or higher-order interactions, such as multiphoton ionization or three-photon absorption, that might use the two-photon transition as an intermediate step.

Our analysis of the effects of transition linewidth to evaluate $\bar{g}G^{(2)}$ was tested by acquiring data both from pure NO at 3 Torr, where Doppler-broadening is dominant, and from 3 Torr of NO in 112 Torr of N_2 , where collisional-broadening is substantial. The influence of N_2 quenching

on the NO $\gamma(0,0)$ fluorescence is known to be negligible¹⁹⁻²¹ so that only broadening effects influenced the observation. Comparing the two cases, the implied ratio of $\bar{g}G^{(2)}$ ranged between 2.0 and 2.3 with an average of 2.18, in good agreement with the predicted ratio of 2.15 listed in Table I for single-mode excitation.

Considering all sources of uncertainty and computing their rms deviation, we obtain the absorptivity, $\alpha_{ul}^{(2)} = 3.0 \pm 1.5 \times 10^{-20} \text{ cm}^2/\text{J}$. Values of the other experimental parameters defining the conditions of our measurement are summarized in Table II. The corresponding matrix element value is $|M_{ul}|^2 = 2.8 \pm 1.4 \times 10^{-51} \text{ cm}^6$, which may be compared with the only other literature value for NO known to us — that of Hochstrasser *et al.*³ Hochstrasser *et al.* reported a value for the O_{12} ($J'' = 6-1/2$) transition in the NO $\gamma(0,0)$ band that was obtained using a three-wave mixing technique designed to be insensitive to the spatial and temporal properties of the incident beams. Using the predicted ratio of relative absorptivity for the two transitions, their measurement implies a value for the $S_{11} + R_{21}$ ($J'' = 7-1/2$) transition of $|M_{ul}|^2 = 0.7 \times 10^{-51} \text{ cm}^6$. Although their measurement is reported without a discussion of the experimental uncertainty, we find the agreement to be satisfying considering the extreme differences in experimental methods.

IV. SUMMARY

Two experiments are reported that combine to quantitatively characterize the two-photon rotational absorption spectrum of the $A^2\Sigma^+(v' = 0) - X^2\Pi(v'' = 0)$ band in nitric oxide. The method used in both experiments is based on the detection of induced broadband fluorescence as a measure of the two-photon absorption.

In the first experiment, a frequency-scanned laser is used to evaluate the relative absorptivities of individual rotational transitions over a wide range of the spectrum. The results are compared with a synthetic spectrum based on an intermediate coupling model for the line-intensity factors. The synthetic spectrum reproduced all of the details of the experiment very well but required the use of recently modified fundamental rotational constants to duplicate the spectral registration of individual lines in overlapping rotational branches, particularly for high initial rotational quantum numbers.

A well-characterized pulse-pumped dye laser system, operating predominantly with a single axial mode, was used in the second experiment to measure the absolute absorptivity of one of the strongest transitions in the NO $\gamma(0,0)$ band. The pertinent experimental parameters and the effects of their uncertainties on the measurement are discussed. When the laser is constrained to just a few statistically independent modes, the uncertainties due to temporal coherence are shown to be small compared with those associated with directly measurable quantities such as the fluorescence energy and the laser power waveform. The requirements on the laser system to allow a measurement to be made with reasonable certainty are found to be manageable, using recently developed pulsed laser concepts. The absorptivity value obtained is in acceptable agreement with the result of a similar measurement in NO in which a greatly different experimental method was used.



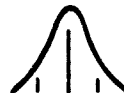
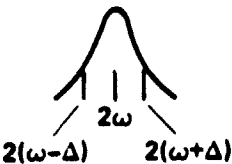
The combined results of both experiments performed in this work allow quantitative estimates of the absorptivity for all two-photon transitions in the NO $\gamma(0,0)$ band.

References

- ¹R. L. McKenzie and K. P. Gross, *Appl. Opt.* 20, 2153 (1981).
- ²J. B. Halpern, H. Zacharias, and R. Wallenstein, *J. Mol. Spectrosc.* 79, 1 (1980).
- ³R. M. Hochstrasser, G. R. Meredith, and H. P. Trommsdorff, *Chem. Phys. Lett.* 53, 423 (1978).
- ⁴R. G. Bray and R. M. Hochstrasser, *Mol. Phys.* 31, 1199 (1976).
- ⁵S. C. Wallace and K. K. Innes, *J. Chem. Phys.* 72, 4805 (1980).
- ⁶R. Wallenstein and H. Zacharias, *Opt. Commun.* 25, 363 (1978). [Note that in Fig. 1 of this reference, the rotational quantum number assignments are given vs $(J'' + 1/2)$.]
- ⁷R. Engleman, Jr., and P. E. Rouse, *J. Mol. Spectrosc.* 37, 240 (1971).
- ⁸R. Freedman and R. W. Nicholls, *J. Mol. Spectrosc.* 83, 223 (1980).
- ⁹J. Ducuing and N. Bloembergen, *Phys. Rev. A* 133, 1493 (1964).
- ¹⁰H. P. Weber, *IEEE J. Quantum Electron.* QE-7, 189 (1971).
- ¹¹I. V. Tomov and A. S. Chirkin, *Sov. J. Quantum Electron.* 1, 79 (1971).
- ¹²J. Krasinski, S. Chudzynski, W. Majewski, and M. Glodz, *Opt. Commun.* 12, 304 (1974).
- ¹³L. G. Dodge, J. Dusek, and M. F. Zabrialski, *J. Quant. Spectrosc. Radiat. Transfer* 24, 237 (1980).
- ¹⁴Y. K. Park and R. L. Byer, *Opt. Commun.* 37, 411 (1981).
- ¹⁵M. G. Littman, *Opt. Lett.* 3, 138 (1978).
- ¹⁶M. K. Iles, A. P. D'Silva, and V. A. Fassel, *Opt. Commun.* 35, 133 (1980).
- ¹⁷R. Wallenstein and T. W. Hensch, *Opt. Commun.* 14, 353 (1975).
- ¹⁸Shardanand and A. D. Prasad Rao, NASA Technical Note D-8442, March 1977.

- ¹⁹A. B. Callear and M. J. Pilling, *Trans. Faraday Soc.* 66, 1618 (1970).
- ²⁰Y. Haas and M. Asscher, in Advances in Chemical Physics, Vol. 47 (XLVII),
Photoselective chemistry, Pt. 2, J. Jortner, R. D. Levine and S. A. Rice,
Eds. (Wiley 1981), p. 17.
- ²¹M. Asscher and Y. Haas, *J. Chem. Phys.* (to be published).
- ²²H. Zacharias, J. B. Halpern, and K. H. Welge, *Chem. Phys. Lett.* 43, 41
(1976).

TABLE I. The effects of laser mode pattern on the two-photon line-shape convolution integral.

Multimode case ^a	$\bar{g}G^{(2)}$ (10^{-10} sec)		
	Doppler	Voigt	Doppler/Voigt ratio
I 	3.13	1.46	2.15
II 	3.07	1.76	1.75
III 	3.33	1.86	1.80
IV 	3.40	2.00	1.70

^aPatterns are shown in order of probability of occurrence.

The transition center frequency is 2ω and Δ denotes the mode spacing. The Voigt function pertains to NO $\gamma(0,0)$ band transitions collision-broadened by 112-Torr N_2 .

TABLE II. Experimental conditions for absorptivity measurement

Transition	$\Lambda^2 \Sigma^+(v' = 0) - X^2 \Pi_{1/2}(v'' = 0)$ $S_{11} + R_{21} (J'' = 7-1/2)$ $N_L/N_T (J'', \Lambda) = 0.024 (300 \text{ K})$ Doppler FWHM = 0.1 cm^{-1} Voigt parameter ^a = 0.87 for 112 Torr N ₂ $\tau_f = 216 \text{ nsec}^b$; $\tau_f/\tau_c = 1.4 \text{ Torr}^{-1}{}^b$
Laser source	$\lambda = 451.75 \text{ nm}$, $\Delta\omega_L \leq 0.02 \text{ cm}^{-1}$ FWHM (single mode) $L = 0.05 \text{ cm}$, $\phi_L \approx 1$ Focal spot diameters: 35 to 85 μm
Absorptivity	$\alpha_{ul}^{(2)} = 3.0 \times 10^{-20} \text{ cm}^4/\text{J}$ $ M_{ul} ^2 = 2.8 \times 10^{-51} \text{ cm}^6$ $\delta = 4.2 \times 10^{-48} \text{ cm}^4\text{-sec/photon}$ for line center of a Doppler-broadened transition at 300 K

^aReference 13.

^bReference 22.

Figure Captions

FIG. 1. Synthetic NO $\gamma(0,0)$ band two-photon excitation spectrum calculated for 300 K and a Gaussian line-shape function with an FWHM bandwidth of 0.5 cm^{-1} (brackets indicate the regions studied).

FIG. 2. Experimental and predicted low-resolution two-photon excitation spectra in the NO $\gamma(0,0)$ R,S region; NO pressure 1 Torr, laser bandwidth 0.3 cm^{-1} .

FIG. 3. Relative rotational line peaks from the NO $\gamma(0,0)$ $S_{11} + R_{11}$ branch at 296 K.

FIG. 4. Experimental and predicted two-photon excitation spectra in the NO $\gamma(0,0)$ O_{12} branch; NO pressure 1 Torr, laser bandwidth 0.5 cm^{-1} .

FIG. 5. Experimental arrangement for the absorptivity measurement:
BS, beam splitter; M, mirror; CL, cylindrical lens; DC1, dye-cell oscillator; DC2, dye-cell amplifier; G, grating (2400 \AA/mm); BE, beam expander; DVP, direct vision prism; PH, pinhole aperture; I, iris; CP, calcite polarizer; FC, fluorescence cell; S, slit; PMT, photomultiplier; PD, photodiode; JM, joulemeter.

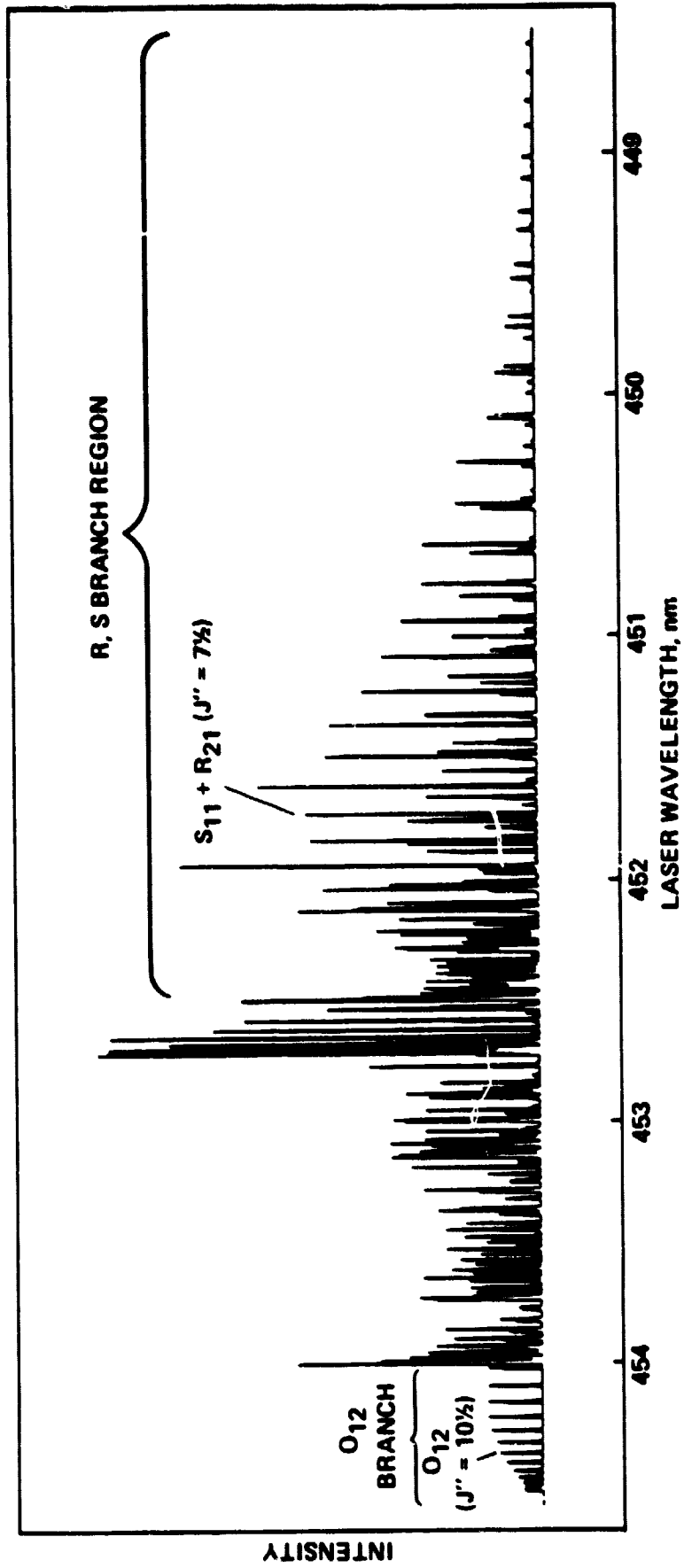


Fig. 1

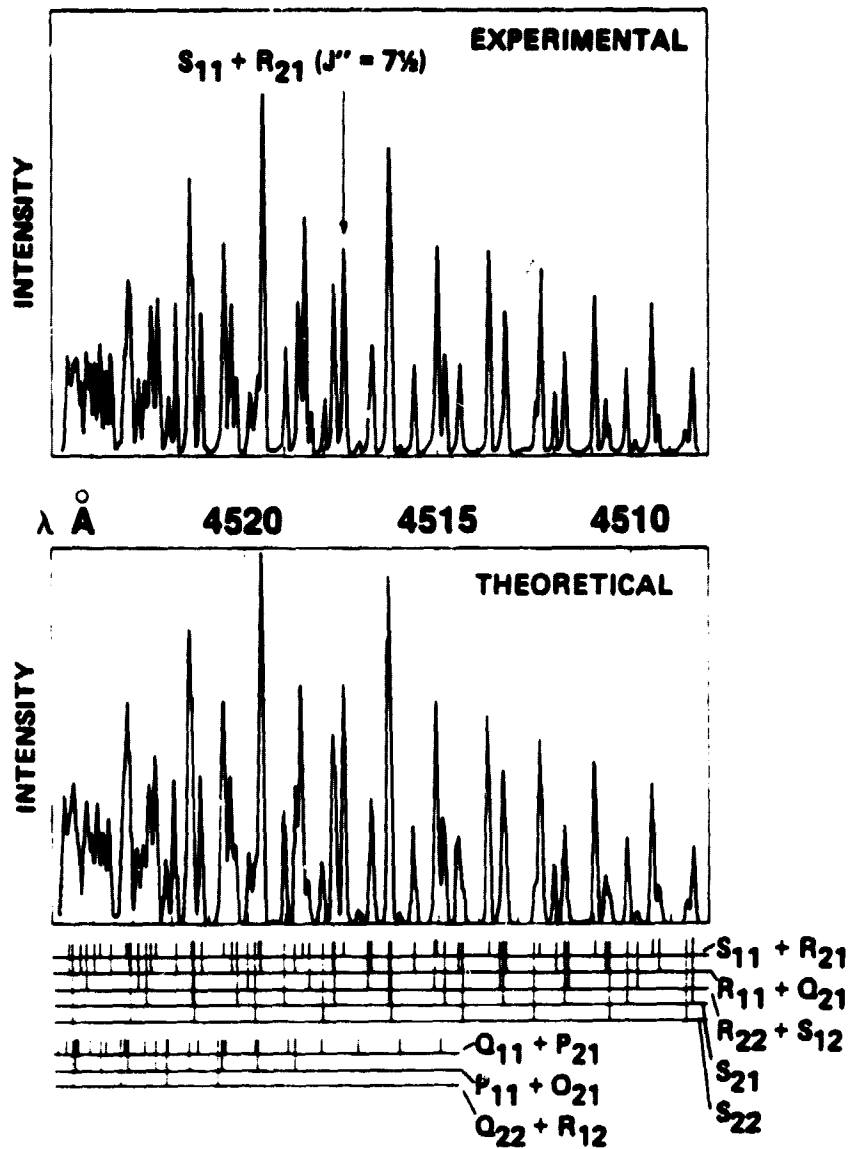


Fig. 2

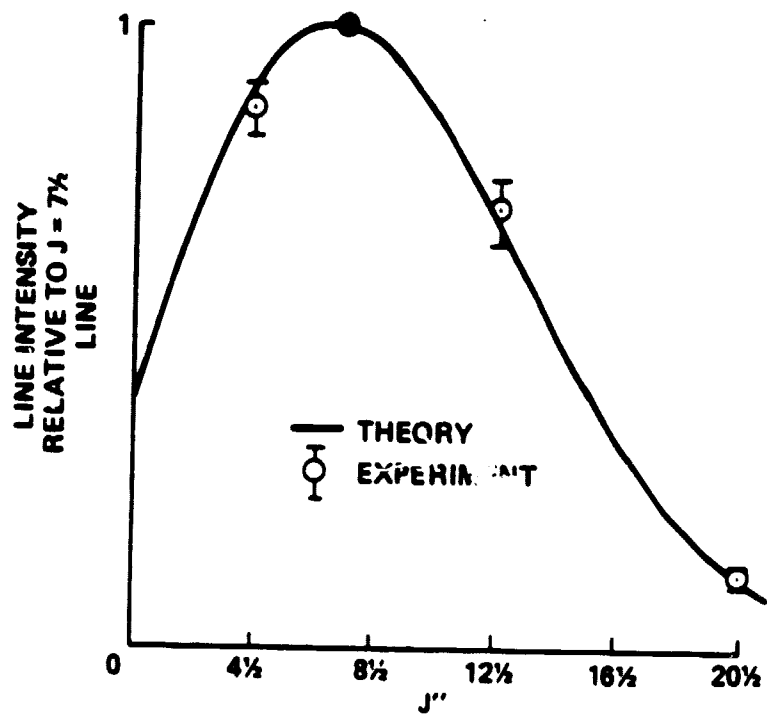


Fig. 3

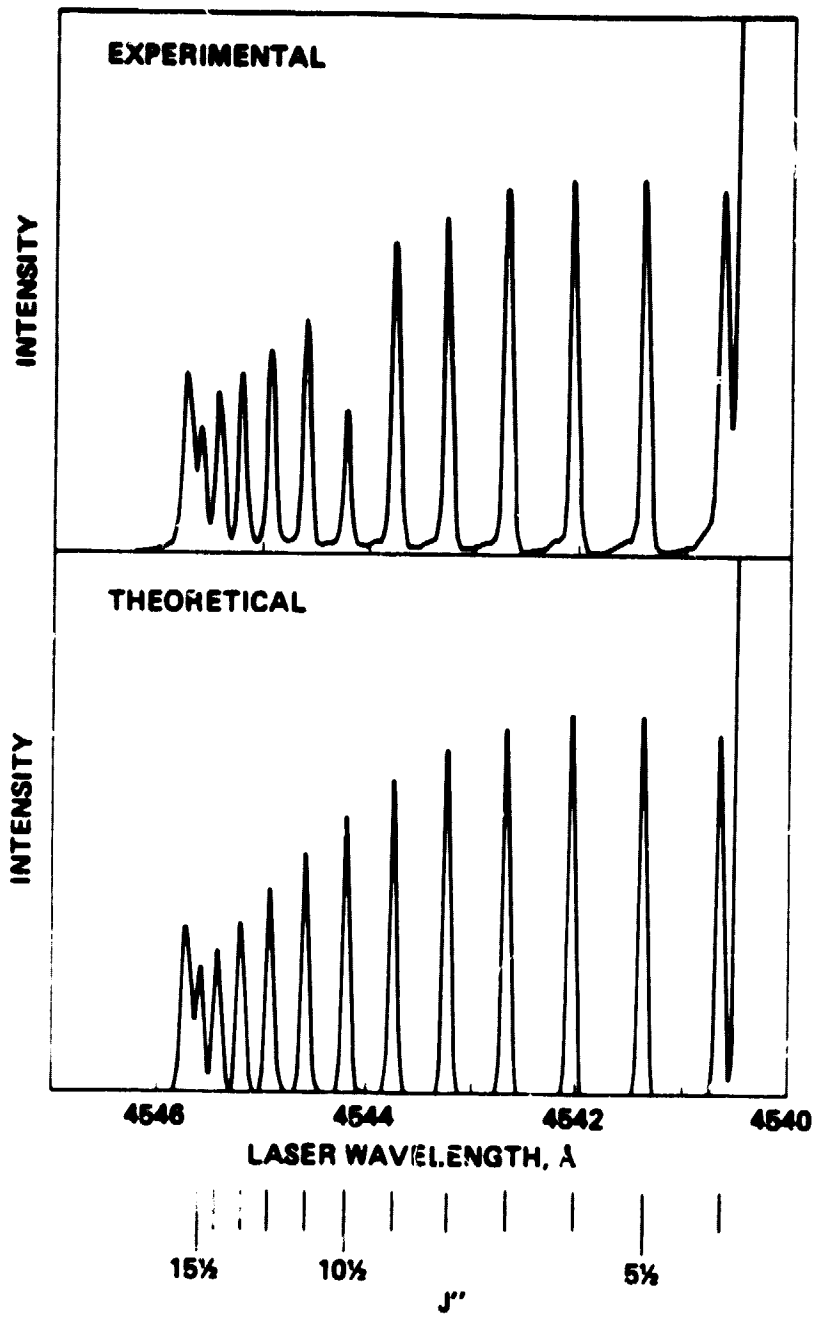


Fig. 4

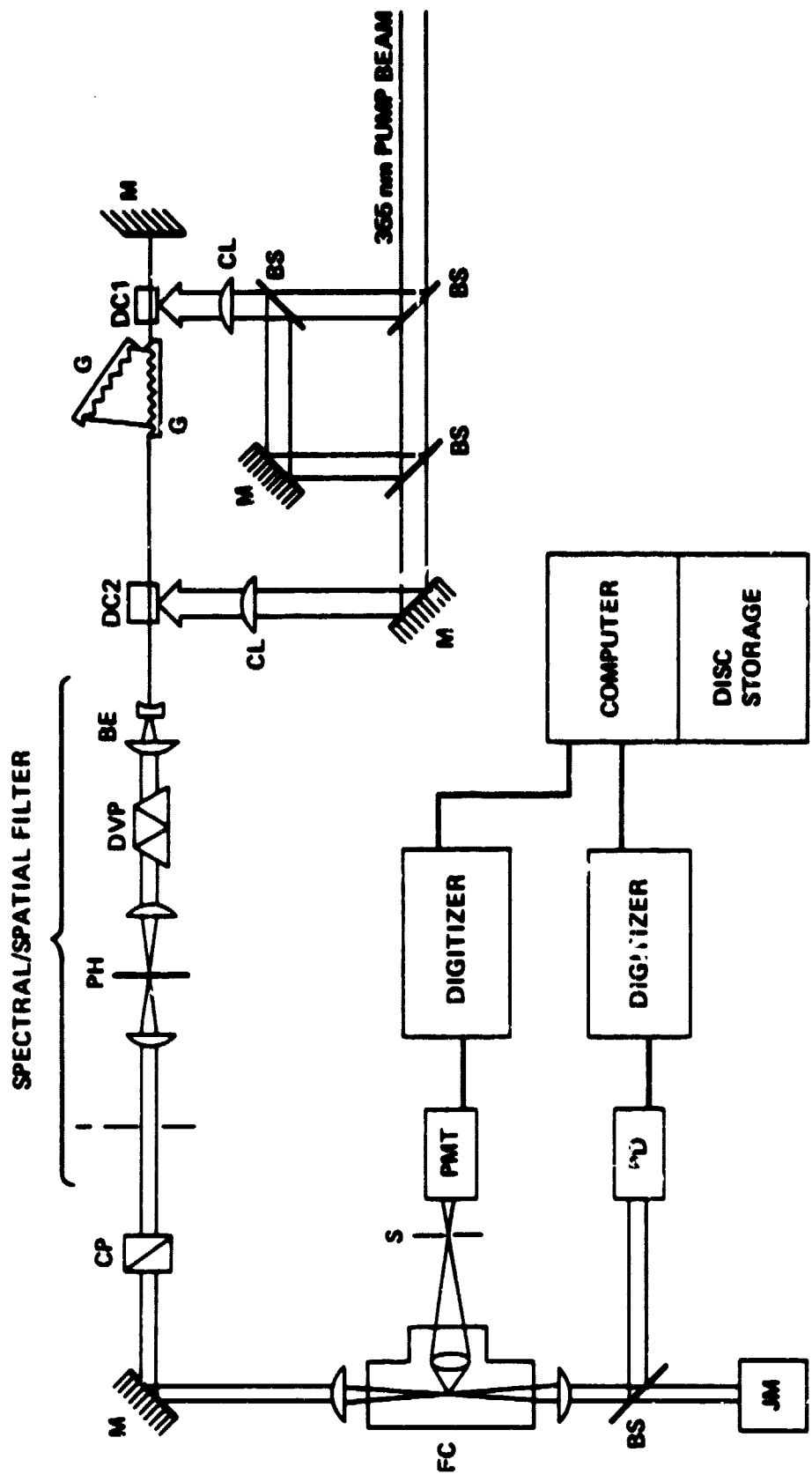


Fig. 5